frontiers in Marine Science

ORIGINAL RESEARCH
published: 28 March 2022
doi: 10.3389/fmars.2022.846914

Shoreline Evolutionary Trends Along Calabrian Coasts: Causes and Classification

Giandomenico Foti[1]*, Giuseppe Barbaro[1], Giuseppina Chiara Barillà[1], Pierluigi Mancuso[2] and Pierfabrizio Puntorieri[1]

[1] Civil, Energy, Environmental and Material Engineering Department (DICEAM), Mediterranea University of Reggio Calabria, Reggio Calabria, Italy, [2] Public Works Department, Catanzaro, Italy

OPEN ACCESS

Edited by:
Roshanka Ranasinghe,
IHE Delft Institute for Water Education, Netherlands

Reviewed by:
Goneri Le Cozannet,
Bureau de Recherches Géologiques et Minières, France
Ali Dastgheib,
IHE Delft Institute for Water Education, Netherlands

***Correspondence:**
Giandomenico Foti
giandomenico.foti@unirc.it

Specialty section:
This article was submitted to Coastal Ocean Processes, a section of the journal Frontiers in Marine Science

Received: 31 December 2021
Accepted: 25 February 2022
Published: 28 March 2022

Citation:
Foti G, Barbaro G, Barillà GC, Mancuso P and Puntorieri P (2022) Shoreline Evolutionary Trends Along Calabrian Coasts: Causes and Classification. Front. Mar. Sci. 9:846914. doi: 10.3389/fmars.2022.846914

The issue of coastal erosion currently affects most of the world's coastal territories. This erosion is generally caused by an alteration of coastal and river dynamics both due to the action of natural factors and to the increase in anthropogenic pressure, mainly observed in the second half of the last century after the end of the Second World War. In the future, this issue may be more affected by climate change. This paper describes the shoreline evolutionary trends at different time scale along the Calabrian coasts, a region in southern Italy, in over 50 sample areas. Calabria represents an interesting case study due to its geomorphological peculiarities and due to its considerable anthropogenic pressures, which have caused extensive erosive processes. In addition, this paper analyzes the main causes of these evolutionary trends and classifies them using a quick methodology based on a shoreline variation rate of a fixed area. This is an index-based methodology and is a part of a new generally index-based coastal risk assessment methodology, developed by the Mediterranea University of Reggio Calabria and the Calabria Region and which is currently in progress. The main result is that the sample areas in the erosion classes prevail over those in the advancement class for very long-term, long-term and middle-term time interval while for short-term and most recent time interval the sample areas in the advancement class prevail over those in the erosion classes.

Keywords: coastal erosion, shoreline changes, coastal risk assessment, index-based methodology, remote sensing, GIS

INTRODUCTION

Coastal erosion processes currently affect most of the world's coastal areas (Luijendijk et al., 2018; Mentaschi et al., 2018). These processes are caused by many natural and anthropogenic factors that alter both coastal and river dynamics (Komar, 2000; Amrouni et al., 2019; Ozpolat and Demir, 2019; Wang et al., 2019; Zhang et al., 2019; Zhai et al., 2020). In fact, the equilibrium of coastal areas is also influenced by the rivers of the same physiographic unit (Acciarri et al., 2016; Barbaro et al., 2019a; Foti et al., 2019).

The main natural factors are the wave climate (Almar et al., 2015; Kroon et al., 2020), the rainfall events (Dada et al., 2015; Zellou and Rahali, 2019), and the coastal sedimentary balance, which is mainly related to longshore and river transport (Barbaro et al., 2014b; Li et al., 2014; Tomasicchio et al., 2015; Dada et al., 2018; Anthony et al., 2019; Besset et al., 2019).

The main anthropogenic factors are the construction of hydraulic structures such as dams and weirs (Zema et al., 2014), the withdrawal of river sediment (Foti et al., 2020a), the destruction of dune systems (Foti et al., 2022) and the construction of ports and coastal defenses (Barbaro, 2013; Prumm and Iglesias, 2016; Valsamidis and Reeve, 2017). Furthermore, anthropogenic pressure causes an increase in impermeable surfaces with negative consequences on the vulnerability of the territory under the action of natural events such as floods and sea storms (Fiori et al., 2014; Barbaro et al., 2020), especially when concurrent events occur (Barbaro et al., 2019b; Canale et al., 2020). Climate change can also contribute to erosive phenomena by the increasing of sea levels and the frequency and intensity of extreme weather events (Santini, 2011; Yang et al., 2015).

Furthermore, erosive processes can occur at different time scales: instantaneous, seasonal, and long-term. The instantaneous variations are related to the wave action and are more relevant during intense sea storms (Harley et al., 2017). Seasonal and annual variations are linked to the wave action, tides, and currents, generally with erosion during the winter and natural nourishment during the summer months (Short and Trembanis, 2004; Thomas et al., 2011; Barnard et al., 2015). Long-term variations are caused by subsidence, tectonic movements, sea level rise due to climate change (Ranasinghe et al., 2004), and changes in coastal and river sedimentary balance due to anthropogenic actions (Turner, 2006; Bird, 2018).

Therefore, coastal areas represent complex dynamical systems and to protect and manage coastal areas various coastal erosion risk assessment methodologies have been defined here (Anfuso and Del Pozo, 2009; McLaughlin and Cooper, 2010; Ramieri et al., 2012; Torresan et al., 2012; Barbaro, 2016; Satta et al., 2016; Jaranovic et al., 2017; Narra et al., 2017; Satta et al., 2017; Kantamaneni et al., 2018; Mavromatidi et al., 2018; Pantusa et al., 2018; Viavattene et al., 2018; Mucerino et al., 2019; Bruno et al., 2020). From this point of view, it is important to analyze coastal and river dynamics, and to estimate and classify shoreline changes (Boak and Turner, 2005; Mills et al., 2005; Maiti and Bhattacharya, 2009; Maanan and Robin, 2010; Williams et al., 2018; Goncalves et al., 2019; Görmüş et al., 2021; Ngowo et al., 2021). A key element in estimating shoreline changes is the cartography data available. These data include historical cartographies, orthophotos, satellite images, and UAV and Lidar (Light Detection and Ranging or Laser Imaging Detection and Ranging) surveys (Le Mauff et al., 2018; Nicolae-Lerma et al., 2019; Mao et al., 2021). Among these, satellite images have been widely used in recent times for three main reasons: they are free available, they interface well with GIS (Geographical Information Systems) and are provided in infrared spectral bands, therefore the water-land interface is well defined (Duarte et al., 2018; Hagenaars et al., 2018; Qiao et al., 2018; Toure et al., 2019; Vos et al., 2019; Konlechner et al., 2020).

This paper describes the shoreline evolutionary trends at different time scale along the Calabrian coasts, a region in southern Italy, in over 50 sample areas. Calabria is a region in Southern Italy that represents an interesting case study due to its geomorphological peculiarities and due to its considerable anthropogenic pressures, which have caused extensive erosive processes (Barbaro et al., 2014a). In addition, this paper analyzes the main causes of these evolutionary trends and classifies them using a quick methodology based on a shoreline variation rate of a fixed area. This is a quick index-based methodology and is a part of a new generally index-based coastal risk assessment methodology which is currently in progress. The new quick methodology completes and improves the work started by Foti et al. (2020b) and improves the methodology developed by Barbaro (2016), proposing an index based on a shoreline variation rate and classifying the shoreline evolutionary trend into 5 classes. This classification was inspired by that proposed by Ferreira Silva et al. (2017), but it differs from it in the definition of the shoreline variation rate which is the novelty of this methodology and is more representative of the shoreline evolutionary trend than the previous methodologies.

MATERIALS AND METHODS

This section is divided into two parts. The first part describes the geomorphological peculiarities of the study area. The second part describes the quick methodology proposed in this paper to classify the shoreline evolutionary trend.

Site Description

Calabria is a region in southern Italy, located at the tip of the typical Italian "boot" in the center of the Mediterranean Sea enclosed by two seas, the Tyrrhenian and the Ionian, by the Strait of Messina and by the Gulf of Taranto, each of them with different climatic characteristics and with different fetch extensions (**Figure 1**). From the morphological point of view, Calabria is characterized by hills and mountains, with a percentage of less than 10% of flat lands. The main massifs are Pollino, Sila, and Aspromonte, all with a maximum altitude of the order of 2000 m. The main coastal plains are that of Sibari, on the Ionian coast in the Gulf of Taranto, and those of Lamezia Terme and Gioia Tauro, both on the Tyrrhenian coast. Its narrow and elongated shape means that it has over 750 km of coastline, with an alternating mainly sandy and pebbly beaches, and high coasts, with the main headlands are those of Capo Rizzuto, on the Ionian coast, and of Capo Vaticano, on the Tyrrhenian coast.

From a climatic point of view, the Ionian coasts are mainly exposed to the winds of Scirocco, South-East, and Grecale, North-East, while the Tyrrhenian coasts are mainly exposed to the winds of the Mistral, North-West. Regarding the fetch extensions, it varies from a few tens of kilometers within the Strait of Messina and the Gulf of Taranto to several hundred kilometers along various directions in the Ionian and Tyrrhenian seas. These differences lead to a remarkable variability of weather and sea conditions between the different coastal areas which influences the coastal dynamics and that cause meteorological events that damage the territory (Canale et al., 2021). Also, tidal excursion is negligible (Sannino et al., 2015).

Most Calabrian rivers (locally called "fiumare") (Sorriso-Valvo and Terranova, 2006; Sabato and Tropeano, 2014), are characterized by a torrential and irregular hydrological regime,

FIGURE 1 | The Calabrian region (shown with red polygon), in the center of the Mediterranean Sea.

with extensive dry periods and frequent sudden flooding, caused by short and intense rainfalls. Also, many of these rivers have very wide beds with coarse grain size. This combination of hydrological and granulometric characteristics causes high solid transport, and the relative variations can alter the coastal dynamics and the shoreline evolution near the river mouths, as shown by Barbaro et al. (2019a) and by Foti et al. (2019) in the case studies of mouths of the Petrace River and Sant'Agata River, respectively.

To analyze the evolutionary trend and the main erosive causes of the Calabrian coasts, over 50 sample areas with different morphological and anthropogenic characteristics were chosen (**Figure 2** and **Table 1**). In most cases, over 40, anthropized areas have been chosen close to inhabited centers while in the remaining areas there are only scattered houses. In over 20 areas there are coastal defense works and over 10 areas are close to ports. Finally, 3 areas are related to pocket beach, in 4 areas there are dune systems, and over 10 are close to river mouths.

Methodology

The methodology proposed in this paper to classify the shoreline evolutionary trend can be divided into eight phases (**Figure 3**):

1. Acquisition of available cartographic data, such as historical shoreline, orthophotos, and satellite images.
2. Manual digitization of each missing shorelines, using QGIS for orthophotos and using Google Earth Pro for satellite images.
3. Choice and tracking of the transepts representative of each sample area, using QGIS.
4. Estimation of the beach width for each transept, using QGIS.
5. Estimation of the shoreline changes for each transept, using end point rate ("EPR") and net shoreline movement ("NSM") statistics.
6. Estimation of the influence area of each transept, using QGIS.
7. Estimation of the shoreline variation rate of each sample area.
8. Classification of the shoreline evolutionary trend of each sample area based on the shoreline variation rate.

Regarding the last two phases, a quick methodology was developed to classify the shoreline evolutionary trend into five classes, based on the value of the shoreline variation rate index v which is the novelty of this methodology. This index was inspired

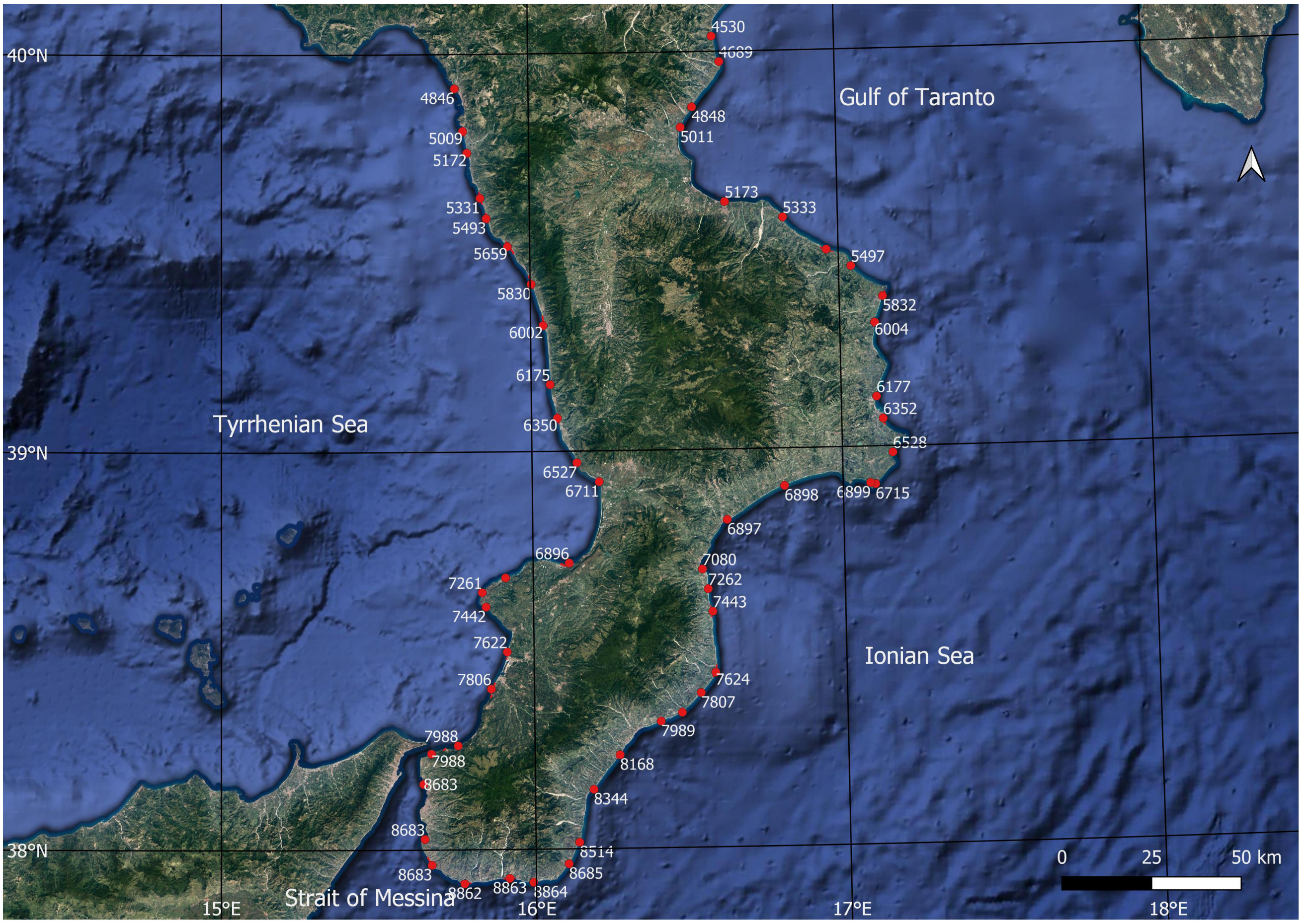

FIGURE 2 | The Calabrian towns examined are identified with a code. Their names are shown in **Table 1**.

by Barbaro's (2016) and this classification was inspired by that proposed by Ferreira Silva et al. (2017).

The shoreline variation rate is calculated with the following formula:

$$\bar{v} = \sum_i v_i \cdot \frac{\Delta A_i}{\Delta A_{tot}}$$

where v_i is the variation rate of the i-th transept evaluated in terms of EPR; ΔA_i is the influence area of the i-th transept, defined as the area between the midpoints of the lines joining the i-th transept with the adjacent ones, and ΔA_{tot} is the sum of the influence areas of all the transepts of the study area. In fact, the shoreline variation rate v is the weighted average shoreline variation rate for each study area, where the weight is given by the influence areas of each transept.

The classes defined by this methodology are advancement ($v > 0.5$), stability ($-0.5 \leq v \leq 0.5$), erosion ($-1 \leq v < -0.5$), intense erosion ($-2 \leq v < -1$), and severe erosion ($v < -2$).

Furthermore, the evaluation of the evolutionary trend of the shoreline was carried out for different timescales as follows: the two most recently available shorelines; a short-term evolutionary trend, with reference to the shorelines available in the last 5 years; a middle-term evolutionary trend, with reference to the shorelines available in the last 20 years; a long-term evolutionary trend, with reference to the shorelines available in the last 30 years; and a very long-term evolutionary trend, with reference to the shorelines available in the past 70 years. For example, with reference to 2020 the time interval would be as follows. Most recent = shorelines of 2020 and 2019; short-term = shorelines from 2016 to 2020; middle-term = shorelines from 2001 to 2020; long-term = shorelines from 1991 to 2020; very long-term = shorelines from 1951 to 2020.

The proposed methodology is more complete than Barbaro's (2016) because it considered the influence area of each transept and because it analyzed the shoreline changes over a time interval of 70 years instead of 15 years, between the 1998–2003, 2003–2008, and 2008–2013 with fixed sub-intervals of 5 years each. However, only a medium-term and a short-term evolutionary trend were analyzed, neglecting a long-term and a very long-term trend. The new methodology has filled this gap. Also, Barbaro's methodology did not analyze evolutionary trends on an annual scale due to the lack of satellite images at that time interval. In fact, only since 2015 are satellite images available on an annual scale for most of the Calabrian coastal areas and this lack was also

TABLE 1 | Sample areas and related code (**Figure 2**).

Sample area	Code	Anthropization	Coastal defense works	Other
Montegiordano	4530	I	G	
Roseto Capo Spulico	4689	I	G	
Trebisacce	4848	I		
Villapiana	5011	S		D
Rossano	5173	I		
Calopezzati	5333	I		
Cariati	5496	I	G	P
Crucoli (Torretta)	5497	I	G	
Cirò Marina	5832	I	B	P
Torre Melissa	6004	I	B	
Crotone (Zigari)	6177	S		
Crotone	6352	I	B	P
Isola Capo Rizzuto (Marinella)	6528	S		PB
Isola Capo Rizzuto	6715	I		
Isola Capo Rizzuto (Le Castella)	6899	S		PB
Cropani	6898	S		D
Catanzaro Lido	6897	I		P
Soverato	7080	I		
San Sostene	7262	S		R
Badolato	7443	S		D, P
Monasterace	7624	I		R
Riace	7807	S		
Caulonia	7990	I		R
Roccella Ionica	7989	I	G	P
Locri	8168	I		
Bovalino	8344	I		
Ferruzzano	8514	S		
Brancaleone	8685	I		
Palizzi	8864	I	B	
Bova Marina	8863	I	B	R
Melito Porto Salvo	8862	I		R
Lazzaro	8683	I	G	
Pellaro	8683	I	G	
Gallico	8683	I	B	R
Porticello	7988	I	M	
Favazzina	7988	I	G	R
Palmi	7806	I		R, P
San Ferdinando	7622	I		R, P
Ricadi (Santa Maria)	7442	I		PB
Capo Vaticano	7261	I	G	R
Tropea	7078	S	G	P
Vibo Marina	6896	I	M	P
Gizzeria	6711	S		D
Falerna	6527	I		
Amantea	6350	I	B	
Belmonte	6175	I		
San Lucido	6002	I	M	
Fuscaldo	5830	I	G	
Cetraro	5659	I	M	P
Sangineto	5493	I	M	
Belvedere	5331	I	M	
Santa Maria del Cedro	5172	S		R
Scalea	5009	I		R
Tortora	4846	I		

B, breakwaters; D, dune systems; G, groynes; I, inhabited center; M, mixed interventions; P, ports; PB, pocket beaches; R, river mouth; S, scattered houses.

filled by the new methodology. In addition, the new methodology differs from that proposed by Ferreira Silva et al. (2017) in the definition of the shoreline variation rate *v*. Finally, the results obtained with the new methodology were compared with those obtained considering the eroded and advanced beach surfaces. This comparison showed that the new methodology was useful, as the results were comparable.

About the other phases, in the first phase various cartography data were compared. In detail, the following have been analyzed: the shapefiles of the historical shorelines of 1954, 1998, 2000, and 2008, taken from the Open Data section of the Calabrian Geoportal[1]; orthophotos of 1989, 1996, 2006, and 2012, taken from the Web Map Service (WMS) of the Open Data section of the Italian Geoportal[2]; and satellite imagery from 2015 to 2020, provided by Google Earth Pro. The shapefile of the shoreline of 1954 has been digitized based on CASMEZ, "*Cassa del Mezzogiorno*," cartography of 1954, in scale 1:10000. The shapefiles of the shorelines of 1998 and 2000 have been digitized based on CTR, "Carta Tecnica Regionale," cartography of 1998 and 2000, both in scale 1:5,000. The shapefile of the shoreline of 2008 has been digitized based on the infrared orthophotos of 2008 in scale 1:5,000. The 1989 and 1996 orthophotos are in black and white, were acquired with a Leica RC30 digital camera and have a scale of 1:10000. The orthophotos of 2006 and 2012 are in color, were acquired with a Leica AD40 digital camera and have a scale of 1:10000. Furthermore, the 2012 orthophotos have pixels of 50 cm. Google satellite images from 2015 to 2020 have variable temporal coverage, from a minimum of three to a maximum of six images depending on the location examined.

Regarding the second phase, the digitalization of each missing shorelines, related to orthophotos and Google satellite imagery, was carried out on a scale of 1:1000 on QGIS and at an eye altitude of 200 m, corresponding to a higher scale, on Google Earth Pro using his spatial analysis tools. The upper limits of the beaches were chosen as the baselines and generally correspond to fixed points such as promenades, roads, and structures or the baseline corresponds with the dune systems in cases where the fixed points are very distant from the beach. About digitization on Google Earth, shorelines and baselines were saved as kml files then saved on QGIS as shapefiles. Baselines were used on QGIS as control points to confirm the accuracy of the procedure.

The digitization phase is characterized by various uncertainties, the main ones concern georeferencing and orthorectification processes, the image resolution, the identification of the wet/dry line or other similar lines, the seasonal cycle of erosion and deposition, and the impact of storms (Boak and Turner, 2005; Hapke et al., 2010). In this phase, uncertainties can be quantified, according to Del Rio and Garcia (2013), through the estimation of the physical component of the error, the scanning error and the georeferencing error. In this case, the reference line chosen was the wet/dry line, the cartography data is all related to the summer period and no storm conditions were observed in any of the data, so the

[1] http://geoportale.regione.calabria.it/opendata, accessed on 15 November 2021.

[2] http://www.pcn.minambiente.it/mattm/servizio-wms/, accessed on 15 November 2021.

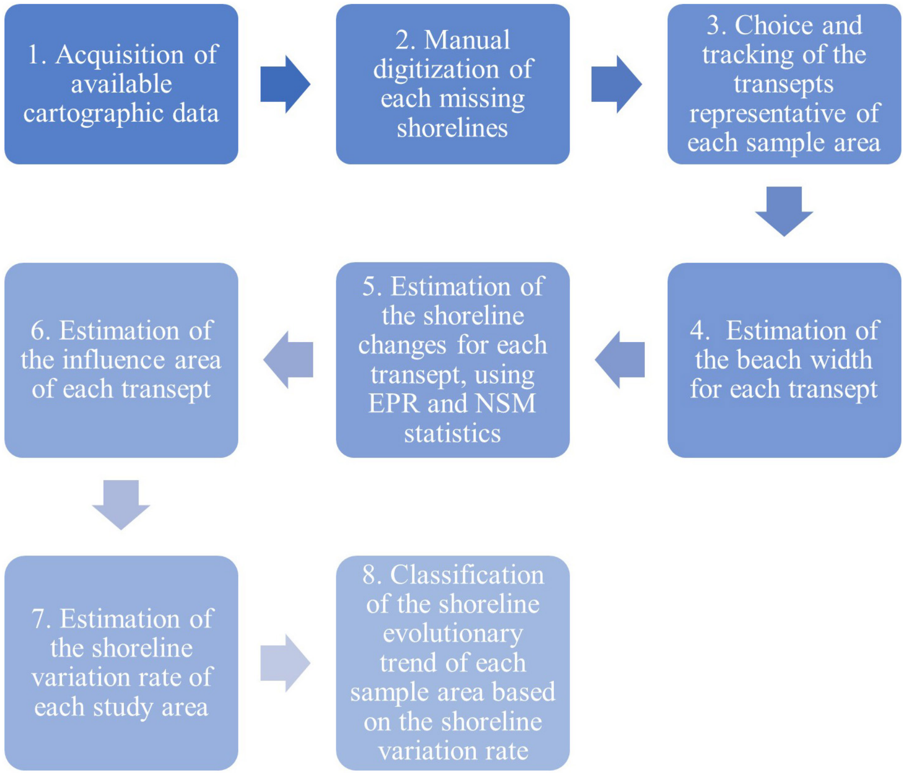

FIGURE 3 | Flow chart of the proposed methodology.

effects of seasonal variation and individual storms on shoreline change are of limited importance. Furthermore, to estimate the tide excursions, the recordings of the tide gages of Crotone and Reggio Calabria were analyzed, the Tide Tables of the Istituto Idrografico della Marina (2020) and the scientific papers were consulted, especially that of Sannino et al. (2015). These sources highlighted that Calabria is a microtidal environment where the tidal excursion is of the order of tens of centimeters. Indeed, the maximum-recorded tide height values are about 25 cm in Reggio Calabria and over 80 cm in Crotone while the minimum recorded tide height values are over −50 cm in Reggio Calabria and over −70 cm in Crotone and the average recorded tide height values are less than 30 cm in Reggio Calabria and about 50 cm in Crotone. Finally, the maximum tide height value reported in the Tide Tables is 25 cm. So, the physical component of the error was estimated using the formula of Allan et al. (2003). The error was estimated, starting from the average and maximum values of the tide height and from the beach slope. This last parameter was estimated using the QGIS Profile tool plugin based on the 1 m side square mesh LIDAR DTMs available on the Italian Geoportal.[3] The beach slope values of the examined locations varied between 1 and 15% so that the estimated error, assuming maximum tide height conditions, was between 1 and 15 m, and the estimated error (assuming minimum tide height conditions) was between 1 and 14 m. However, these are very precautionary values, as the times of the satellite image was not known and, consequently, it is not possible to know the tide conditions at these times. Additionally, the cartography and orthophotos scales are all 1:10000 or less so the scanning errors are of the order of one meter for orthophotos on a scale of 1:10000 and is less than one meter for other sources with a lower scale. On the other hand, regarding the georeferencing error of the Google Earth shorelines, the use of baselines as control points contained the error within a few tens of cm. Finally, since the aim of the paper is the evaluation of the erosion and advancement trends, and not their precise quantification, an accuracy of the order of one meter was considered for estimating the shoreline position and the shoreline changes.

In the third and fourth phases, both developed on QGIS, over 700 transepts representative of each study area were traced. For the choice of the tracing points of the transepts, the following criterion was followed: in the straight and regular beaches an average spacing of the order of a hundred meters was considered, but this was reduced in the presence of coastal structures and in the case of irregular morphologies. Also, for each transept, the distance between the baseline and the shorelines was determined. To automate this process, a point was first inserted at the intersection between each transept and the various shorelines using the line intersection tool. Then, the shortest line function which allows the calculation of the minimum distance between a point and a straight line is used to determine the width of each transept, considering each baseline as straight line.

[3]http://www.pcn.minambiente.it/mattm/, accessed on 15 November 2021.

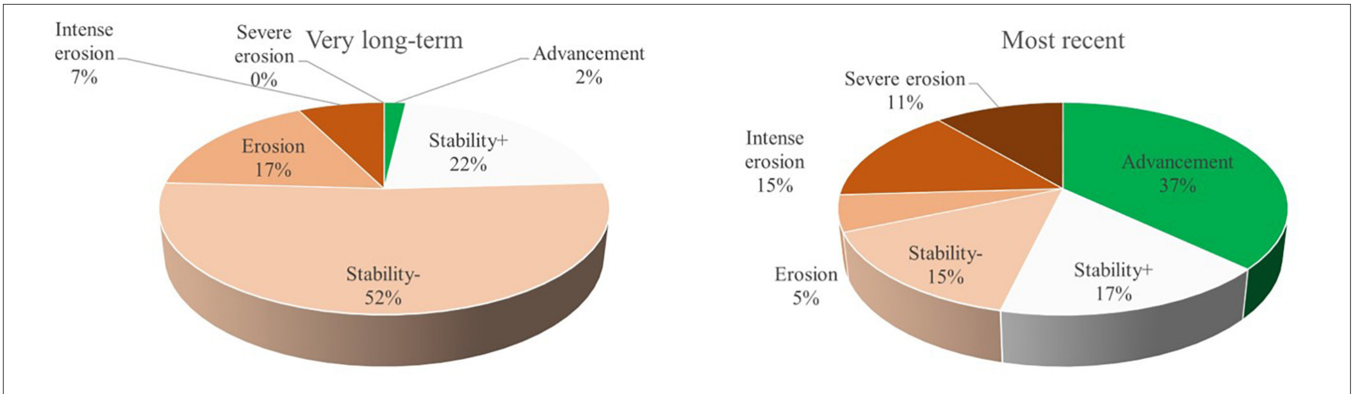

FIGURE 4 | On the **(left)** very long-term shoreline evolutionary trend. To the **(right)** most recent shoreline evolutionary trend.

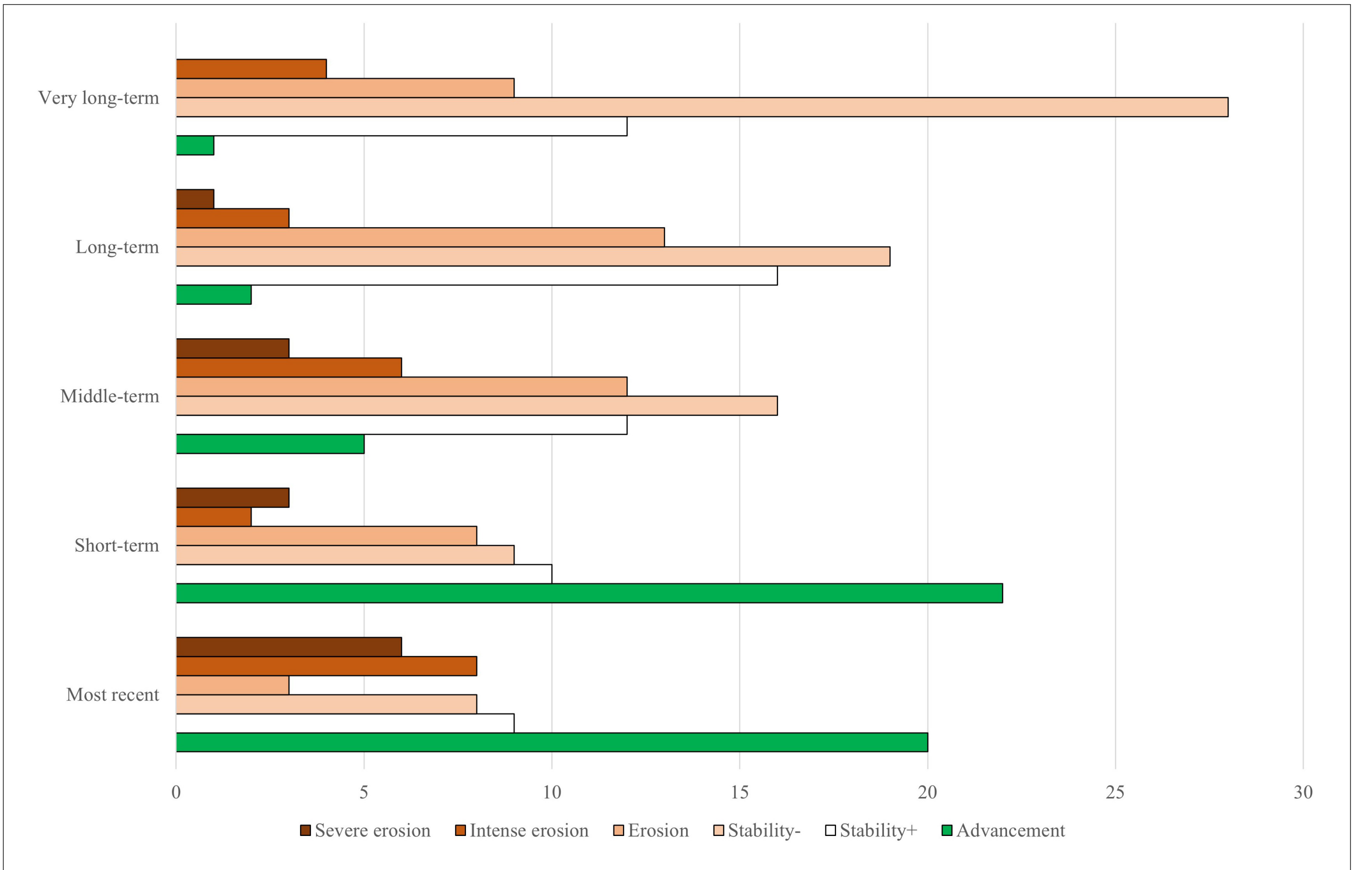

FIGURE 5 | Summary of shoreline evolutionary trends.

For the fifth phase, the NSM and EPR between any two shorelines were calculated. To assess the evolutionary trend of each study area these parameters were also calculated at different time scales being the last 70 years, 30 years, 20 years, 5 years, and finally between the two most recent shorelines available.

Finally, for the sixth phase, QGIS Processing tools were used firstly to draw orthogonal lines to each transept that connect them. The influence area of each transept is the area between the midpoints of the lines joining the examined transept with the adjacent ones and has been calculated using the field calculator.

RESULTS

Tables 2, **3** show a summary of the evolutionary trend for over 50 Calabrian sample areas, according to the classification shown in the previous paragraph. In detail, **Table 2** shows the shoreline evolutionary trend of each sample area while **Table 3** shows the summary of the shoreline evolutionary trends for all areas. In the latter table, the stability class, characterized by both positive and negative shoreline variation rates with values between −0.5 and 0.5 m/year, has been divided into

TABLE 2 | Shoreline evolutionary trend of each sample area.

Sample area	Code	Average shoreline variation rate, *v* [m/year]				
		Most recent	**Short-term**	**Middle-term**	**Long-term**	**Very long-term**
Montegiordano	4530	−0.22	0.21	0.60	0.16	−0.16
Roseto Capo Spulico	4689	0.19	1.93	0.24	0.10	0.12
Trebisacce	4848	0.07	0.07	−0.35	−0.03	0.14
Villapiana	5011	2.21	2.21	0.53	0.37	0.46
Rossano	5173	−0.26	0.16	0.12	−0.10	−0.12
Calopezzati	5333	−3.19	−0.69	−0.67	−0.55	−0.42
Cariati	5496	0.84	−1.10	−0.39	−0.61	−0.29
Crucoli (Torretta)	5497	−2.11	1.04	−0.96	−0.88	0.12
Cirò Marina	5832	−0.36	−0.08	−1.16	−0.77	−0.38
Torre Melissa	6004	0.16	0.80	0.26	0.01	0.11
Crotone (Zigari)	6177	2.18	−3.58	−1.19	−1.44	−1.29
Crotone	6352	0.54	−0.06	−0.66	0.03	−0.23
Isola Capo Rizzuto (Marinella)	6528	0.25	−0.26	−0.46	−0.17	0.05
Isola Capo Rizzuto	6715	−0.90	2.07	−0.61	−0.14	−0.05
Isola Capo Rizzuto (Le Castella)	6899	−0.04	0.46	−0.49	−0.51	−0.25
Cropani	6898	−1.18	2.50	−0.25	0.21	−0.10
Catanzaro Lido	6897	2.34	0.79	0.07	−0.08	−0.38
Soverato	7080	0.97	2.02	0.13	−0.06	−0.24
San Sostene	7262	0.35	−0.65	−0.68	−0.88	−0.57
Badolato	7443	0.16	1.72	1.04	−0.02	0.63
Monasterace	7624	−1.61	1.19	−0.10	−0.34	−0.77
Riace	7807	0.34	1.40	0.06	0.05	0.2
Caulonia	7990	−5.70	−0.57	−1.04	−1.84	−1.65
Roccella Ionica	7989	1.96	1.48	−0.56	−0.15	−0.06
Locri	8168	−1.04	−0.95	−0.56	−0.26	−0.21
Bovalino	8344	−0.72	−0.16	−0.60	−0.20	−0.33
Ferruzzano	8514	−1.15	−0.37	0.17	0.09	0.01
Brancaleone	8685	−2.09	−0.81	−0.19	−0.17	−0.18
Palizzi	8864	−1.37	0.81	0.26	0.26	−0.31
Bova Marina	8863	−1.84	−0.38	−1.23	−0.87	−0.27
Melito Porto Salvo	8862	−1.03	−0.61	−2.14	−0.96	−0.82
Lazzaro	8683	−0.03	−0.15	−1.15	−0.66	−0.26
Pellaro	8683	0.67	0.30	0.01	−0.15	0.02
Gallico	8683	−0.22	−0.30	−0.25	0.10	−0.36
Porticello	7988	−0.13	0.16	−0.92	−0.12	−0.08
Favazzina	7988	0.21	0.51	−0.25	−0.59	−0.14
Palmi	7806	−0.38	1.33	−0.01	−0.27	−0.96
San Ferdinando	7622	−3.06	−0.66	−0.05	0.01	−0.66
Ricadi (Santa Maria)	7442	1.41	0.08	−0.58	−0.21	−0.14
Capo Vaticano	7261	0.90	−1.84	0.12	0.01	−0.48
Tropea	7078	2.79	0.72	0.92	0.82	0.07
Vibo Marina	6896	2.05	0.48	0.69	0.32	−1.82
Gizzeria	6711	−1.63	−5.49	−1.05	0.60	0.38
Falerna	6527	12.10	8.88	−2.98	−2.37	−0.61
Amantea	6350	−0.84	−0.84	−0.74	−0.68	−0.79
Belmonte	6175	−2.81	−2.81	−0.28	0.48	−0.30
San Lucido	6002	0.20	0.20	−0.15	−0.16	−0.19
Fuscaldo	5830	1.21	0.51	−2.06	−1.56	−0.60
Cetraro	5659	3.59	0.87	−0.42	0.04	−0.79
Sangineto	5493	1.30	0.33	−0.77	−0.32	−1.24
Belvedere	5331	1.73	0.67	−0.23	−0.84	−0.32
Santa Maria del Cedro	5172	2.68	1.32	0.06	−0.23	−0.42
Scalea	5009	2.02	1.74	0.26	0.11	0.29
Tortora	4846	4.17	−0.01	−0.09	−0.69	−0.74

Green, advancement; White, stability; Light brown, erosion; Brown, intense erosion; Dark brown, severe erosion.

TABLE 3 | Summary of shoreline evolutionary trend.

Classification/time interval	Most recent	Short-term	Middle-term	Long-term	Very long-term
Advancement	20	22	5	2	1
Stability	17	19	28	35	40
Erosion	3	8	12	13	9
Intense erosion	8	2	6	3	4
Severe erosion	6	3	3	1	0
Advancement, Stability+	29	32	17	18	13
Erosion, Intense Erosion, Severe Erosion	17	13	21	17	13
Erosion, Intense Erosion, Severe Erosion, Stability-	25	22	37	36	41

The color scheme is the same as in ***Table 2****.*

FIGURE 6 | Shoreline erosions near river mouths. red line = shoreline of 1954; background = most recent Google satellite images.

two sub-classes: stability+, where only the positive values have been considered, and stability−, where only the negative values were considered.

These tables show that most of the sample areas are characterized by evolutionary trends that vary depending to the time scale analyzed and only a few sample areas are characterized by evolutionary trends always of the same class. In the latter case, only 5 sample areas are included, where the shoreline evolutionary class is always stability with alternation of stability+ and stability− sub-classes between the various time intervals. Instead, in 6 sample areas, only positive values of the shoreline variation rates are observed, with alternation of advancement and stability+ classes between the various time intervals, and in other 6 sample areas, only advancement and stability classes are observed in all time intervals. On the other hand, in 6 sample areas, there are only erosion and stability classes in all time intervals and in 7 sample areas, only negative values of the shoreline variation rates are observed, with alternation of stability−, erosion, intense erosion and severe erosion classes between the various time intervals, while in 3 sample areas, Caulonia, Melito Porto Salvo, and Amantea, there are only the three erosion classes without the stability− class in all time

FIGURE 7 | Roseto Capo Spulico. **(Large panel)** Baseline (black line) and shorelines of 1954 (red line), 1989 (yellow line), 2000 (green line), and 2006 (brown line) with background Google satellite image of August 2019. **(Small panel)** Overlap between 1954 CASMEZ cartography and Google satellite image of August 2019.

intervals. Finally, in 21 sample areas, both the advancement and the erosion classes are present. Among these sample areas should be mentioned Cariati and Crotone (Zigari), both in the advancement class in most recent but with only negative values of the shoreline variation rates in all other time intervals, with greater values in Crotone (Zigari). Falerna, on the other hand, is largely in the advancement class in the most recent and in the short-term intervals but with strongly negative values of the shoreline variation rates in all the other time intervals. Finally, in various sample area in the Tyrrhenian coast (Fuscaldo, Cetraro, Sangineto, Belvedere, and Tortora), trends like that of Falerna, but with lower values of shoreline variation rates, are observed. This condition of advancement in the most recent and in the short-term intervals and of erosion in the long-term and in the very long-term time intervals does not imply that the current shoreline is in an advanced position compared to that of the 1950s but simply indicates that, after decades of retreat, the shoreline has recently advanced.

Regarding the shoreline variation rates values, there are significant variations depending on the time interval analyzed. In fact, for very long-term the maximum and minimum values are 0.63 m/year in Badolato and −1.82 m/year in Vibo Marina, respectively. For long-term, the maximum and minimum values are 0.82 m/year in Tropea and −2.37 m/year in Falerna. For middle-term, the maximum and minimum values are 1.04 m/year in Badolato and −2.98 m/year in Falerna. For short-term, the maximum and minimum values are 8.8 m/year in Falerna and −5.49 m/year in Gizzeria. Finally, for most recent the maximum and minimum values are 12.1 m/year in Falerna and −5.7 m/year in Caulonia. Among these results, it should be highlighted the case of Badolato, which reaches the maximum values among all the sample areas both for very long-term and for middle-term, and, above all, the case of Falerna, which reaches both the maximum values, for short-term and most recent, that the minimum values, for long-term and middle-term, among all sample areas.

From a temporal point of view, the sample areas in the erosion classes prevail over those in the advancement class for very long-term, long-term and middle-term while for short-term and most recent the sample areas in the advancement class prevail over those in the erosion classes (**Figures 4**, **5**). Instead, the sample areas in the stability class decrease as the time interval decreases. In fact, for very long-term just 1 sample area is in the advancement class while 13 sample areas are in the erosion classes and 40 sample areas are in the stability class, 12 of which are in the stability+ class and the other 28 are in the stability− class.

FIGURE 8 | Villapiana. **(Large panel)** Baseline (black line) and shorelines of 1954 (red line), 1989 (yellow line), 2000 (green line), and 2012 (orange line) with background Google satellite image of October 2019. **(Small panel)** Overlap between 1954 CASMEZ cartography and Google satellite image of October 2019.

For long-term, the sample areas in the advancement class are 2, the sample areas in the erosion classes are 17 and the sample areas in the stability class are 35, 16 of which are in the stability+ class and the other 19 are in the stability− class. For middle-term, the sample areas in the advancement class are 5, the sample areas in the erosion classes are 21 and the sample areas in the stability class are 28, 12 of which are in the stability+ class and the other 16 are in the stability− class. For short-term, the sample areas in the advancement class are 22, the sample areas in the erosion classes are 13 and the sample areas in the stability class are 19, 10 of which are in the stability+ class and the other 9 are in the stability− class. Finally, for most recent time interval the sample areas in the advancement class are 20, the sample areas in the erosion classes are 17 and the sample areas in the stability class are 17, 9 of which are in the stability+ class and the other 8 are in the stability− class.

DISCUSSION

The results described in the previous section show that the sample areas in the erosion classes prevail over those in the advancement class for very long-term, long-term and middle-term while for short-term and most recent the sample areas in the advancement class prevail over those in the erosion classes. These results were analyzed considering both natural and anthropogenic driving factors which influencing shoreline changes, such as the wave climate, the expansion of the inhabited centers with distruction of dune systems and alteration of landward of the beach, and the construction of ports and hydraulic works. Firstly, a general analysis of these factors was carried out. Subsequently, some sample areas where the effects of these driving factors are more representative have been analyzed in detail.

Regarding the wave climate, the peculiar morphology of Calabria exposes it to very different climatic conditions between the Ionian and the Tyrrhenian coasts. Indeed, the Ionian coasts are mainly exposed to the winds of Scirocco, from South-East, and Grecale, from North-East, while the Tyrrhenian coasts are mainly exposed to the winds of the Mistral, from North-West. Also, the fetch extensions vary from a few tens of kilometers within the Strait of Messina and the Gulf of Taranto to several hundred kilometers along various directions in the Ionian and Tyrrhenian seas. These differences lead to a significant variability of sea storms conditions between the various coastal areas which

FIGURE 9 | Badolato. **(Large panel)** Baseline (black line) and shorelines of 1954 (red line) with background Google satellite image of June 2019. **(Small panel)** Overlap between 1954 CASMEZ cartography and Google satellite image of June 2019.

influences the coastal dynamics. In general, the significant wave heights in the Tyrrhenian Sea reach higher maximum values than in the Ionian Sea but in the Tyrrhenian Sea the sea storms are almost entirely concentrated around the sectors coming from the North-West directions while in the Ionian Sea the sea storms can come from a wide range of sectors, from the South-West to North-East directions.

About anthropogenic driving factors, in the second half of the last century, after the end of the Second World War, many of the Calabrian inhabited centers have considerably expanded, especially near the sea. One effect of this expansion is the reduction of the dune systems extension, that is currently equal to one fifth of that of the 1950s. Consequently, in all coastal municipalities where the dune systems were totally destroyed between the 1950s and today and have been replaced by buildings, infrastructures, promenades, etc., coastal erosion processes are observed (Foti et al., 2022). Another important effect of the expansion of the inhabited centers near the sea concerns the alteration of landward of the beach. In fact, like to dune systems, in many locations the new settlements have been built directly on the beach, significantly reducing their width, as in the case of Tortora which will be shown in detail below. Another anthropogenic driving factor concerns the construction of ports. In fact, in Calabria there are currently about twenty ports, just six of which were also present in the 1950s. In addition, in the post-war period the anthropogenic pressure also affected various Calabrian rivers where many hydraulic works were built such as weir, dams, etc. This works has immobilized significant quantities of sediments especially in the valley parts of the river basins, causing significant shoreline retreats near the river mouths. In fact, a peculiarity of Calabrian rivers is high solid transport, whose variations can alter the coastal dynamics and the shoreline evolution near the river mouths, as shown by Barbaro et al. (2019a) and by Foti et al. (2019) in the case studies of mouths of the Petrace River and of the Sant'Agata River, respectively. The rivers with the greatest retreats near the mouth, comparing the shoreline of the 1950s with the more recent one, are Mesima (over 300 m) near San Ferdinando, and Melito, near Melito Porto Salvo, Petrace, near Palmi, and Allaro, near Caulonia (all three over 200 m) (**Figure 6**). Furthermore, in about 20 Calabrian rivers the maximum retreat exceeds 100 m.

It should be noted that most of the anthropogenic driving factors, such as inhabited center and hydraulic works, date back to the first decades after the end of the Second World War.

FIGURE 10 | Caulonia. **(Large panel)** Baseline (black line) and shorelines of 1954 (red line), 1989 (yellow line), and 2000 (green line) with background Google satellite image of June 2019. **(Small panel)** Overlap between 1954 CASMEZ cartography and Google satellite image of June 2019.

In addition, the very long-term and the long-term trends show a prevalence of erosions or stability and only Badolato shows advancement. As will be better described below, the advancement observed in Badolato is related to the construction of a port, therefore the key factors for understanding the very long-term and the long-term evolutionary trends are anthropogenic.

On the other hand, in the new century the construction of new settlements near the sea with alteration of landward of the beaches, the expansion of existing inhabited centers and the construction of new hydraulic works has significantly reduced compared to the previous period. An important consequence of these reductions is that the amount of sediments immobilized in the river basins is also reduced and the amount of sediments that can reach the river mouths can increase. In addition, the short-term and the most recent trends show a prevalence of advancement. This consideration allows us to hypothesize that the short-term and the most recent trend are mainly related to natural factors that alter the sedimentary balance, such as the action of single sea storms or particularly rainy or dry periods.

Finally, it is useful to consider the possible effects of climate change through an analysis of sea level rise according to IPCC (2013), Nerem et al. (2018), Barbaro et al. (2020), and IPCC (2021). These studies show that the average sea level rise is expected to be about 10 cm in the next 20 years, and about 80 cm in the next 100 years. It should be noted that these are estimated values, affected by various uncertainties and which can be exceeded in the presence of worst-case or even catastrophic scenarios, such as the Antarctic collapse. Considering the beach slope values described above, in most of the sample areas this estimated sea level rise would cause linear retreats of the shorelines of the order of a few tens of meters in the next 100 years. Therefore, even in the absence of worst-case or catastrophic scenarios, these retreats can have a significant impact on the Calabrian coasts.

Some sample areas were analyzed in detail below.

Roseto Capo Spulico is a town in the Gulf of Taranto where the shoreline variation rate is always positive and is an example of an advanced shoreline due to the construction of coastal defense works. In fact, until 2006 the beach width was less than 20 m, with modest variations in the shoreline over the years. Between 2006 and 2012 some groynes were built which caused a beach advance by several tens of meters, up to a maximum of 70 m (**Figure 7**).

Villapiana is another town in the Gulf of Taranto where the shoreline variation rate is always positive and the most recent,

FIGURE 11 | Falerna. **(Large panel)** Baseline (black line) and shorelines of 1954 (red line), 2000 (green line), and 2017 (yellow line) with background Google satellite image of June 2019. **(Small panel)** Overlap between 1954 CASMEZ cartography and Google satellite image of June 2019.

short-term and middle-term trend is advancement. Villapiana is one of the few places where the expansion of the inhabited center took place almost entirely behind the existing dune system and the shoreline is currently advanced up to 30 m compared to that of the 1950s (**Figure 8**).

Badolato is a town of the Ionian Sea whose coastal dynamics have been significantly modified, at the beginning of this century, by the construction of a port in a straight coastal area with high longshore transport, as also shown in previous research (Miduri et al., 2017). Indeed, the analysis of the historical shorelines shows a relevant advance south of the port, with maximum value of about 170 m compared to the shoreline of 1950s, with considerable erosion to the north of the port and with periodic obstructions of the port mouth. The advance and the erosion areas are of the same order of magnitude, so they are balanced, as shown in **Table 2**, and the shoreline variation rate always in advance (**Figure 9**).

Caulonia is a town in the Ionian Sea near the mouth of the Allaro river, which is one of the Calabrian rivers at whose mouth the greatest shoreline retreat has been observed, with a maximum value over 200 m compared to the shoreline of 1950s. These retreats affected about 5 km of coastline, both to the left and to the right of the river mouth, causing the destruction of extensive dune systems (**Figure 10**).

Figure 11 shows the very irregular evolutionary trend of Falerna analyzed in the previous section. This trend is caused by anthropogenic pressure through an alteration of landward of the beach. In detail, between 1954 and 1989 shoreline advancement of up to 70 m are observed. In this period, the inhabited center expanded exclusively behind the promenade, which already existed in 1954. Instead, between 1989 and 2006 a shoreline retreat was observed, with a maximum value of about 60 m in the northern part of the inhabited center. In this period some buildings have been built as well as some parking lots instead of portions of the beach. The process of shoreline retreating continued until 2014, especially in the southern part of the inhabited center, with a maximum value exceeding 100 m respect to 1989. Between 2014 and 2017 there was a stability phase, followed by a new shoreline advancement, especially in the southern part of the inhabited center, with a maximum value exceeding 60 m.

Finally, Tortora represents another example of erosive processes caused by anthropogenic pressure like Falerna. In the 1950s, in fact, the town of Tortora was located only in the

FIGURE 12 | Tortora. **(Large panel)** Baseline (black line) and shorelines of 1954 (red line) with background Google satellite image of October 2019. **(Small panel)** Overlap between 1954 CASMEZ cartography and Google satellite image of October 2019.

hills, while on the coast, there was an extensive dune system, with only a few sporadic buildings. Currently, instead of the dune system, the Tortora Marina town has been built, with a promenade and several buildings built not far from the shoreline. Moreover, the beach width is between 30 and a few meters, decreasing toward the north, and a maximum erosion of about 100 m is observed compared to 1954 (**Figure 12**). In recent years, shoreline advancement has been observed especially in the southern part, which explain the irregular evolutionary trend shown in **Table 2**.

CONCLUSION

The paper describes the shoreline evolutionary trends at different time scale along the Calabrian coasts, a region in southern Italy, in over 50 sample areas with different morphological and anthropogenic characteristics such as presence of inhabited centers, scattered houses, ports, coastal defense works, pocket beach, dune systems, and river mouths. The choice of Calabria as a case study is related to its geomorphological peculiarities and due to its considerable anthropogenic pressures, which have caused extensive erosive processes. In addition, this paper analyzes the main causes of these evolutionary trends and classifies them using a quick index-based methodology for classifying the shoreline evolutionary trend into five classes: advancement, stability, erosion, intense erosion, severe erosion. The new methodology differs from the previous methodologies in the definition of the shoreline variation rate of a fixed area that depends on the variation rate of each transept, evaluated in terms of EPR, on the influence area of each transept and of the sum of the influence areas of all the transepts of the fixed area.

The main result is that the sample areas in the erosion classes prevail over those in the advancement class for very long-term, long-term and middle-term time interval while for short-term and most recent time interval the sample areas in the advancement class prevail over those in the erosion classes. The temporal variability of the evolutionary trend may be related to the considerable anthropogenic pressures that occurred in the second half of the last century for very long-term and long-term time interval, and to natural factors for short-term and most recent time interval.

Future developments of this methodology are foreseen. Indeed, annual updates are needed to consider the new Google satellite images available. Also, this methodology is part of a new generally index-based coastal risk assessment methodology, developed by the Mediterranea University of Reggio Calabria and the Calabria Region and which is currently in progress. Finally, this methodology is of interest in the field of coastal area planning and management and is easily applicable in any other context as it leads to the rapid analysis of cartographic data from different sources using remote sensing and GIS free software.

DATA AVAILABILITY STATEMENT

The original contributions presented in the study are included in the article/supplementary material, further inquiries can be directed to the corresponding author.

AUTHOR CONTRIBUTIONS

GF, GB, and GCB: conceptualization and data curation. GF, GB, GCB, PM, and PP: methodology, validation, writing—review and editing, and visualization. GF and GCB: software and writing—original draft preparation. GF, GCB, and PM: formal analysis and investigation. GB and PM: resources, supervision, and project administration.GB: funding acquisition. All authors have read and agreed to the published version of the manuscript.

FUNDING

This work was funded by the Public Works Department of Calabria Region.

REFERENCES

Acciarri, A., Bisci, C., Cantalamessa, G., and Di Pancrazio, G. (2016). Anthropogenic influence on recent evolution of shoreline between the Conero Mt. and the Tronto R. mouth (southern Marche. Central Italy). *Catena* 147, 545–555. doi: 10.1016/j.catena.2016.08.018

Allan, J. C., Komar, P. D., and Priest, G. R. (2003). Shoreline variability on the high-energy Oregon coast and its usefulness in erosion-hazard assessments. *J. Coast. Res.* 38, 83–105.

Almar, R., Kestenare, E., Reyns, J., Jouanno, J., Anthony, E., Laibi, R., et al. (2015). Response of the Bight of Benin (Gulf of Guinea, West Africa) coastline to anthropogenic and natural forcing, Part 1: wave climate variability and impacts on the longshore sediment transport. *Cont. Shelf Res.* 110, 48–59. doi: 10.1016/j.csr.2015.09.020

Amrouni, O., Hzami, A., and Heggy, E. (2019). Photogrammetric assessment of shoreline retreat in North Africa: anthropogenic and natural drivers. *ISPRS J. Photogramm. Remote Sens.* 157, 73–92. doi: 10.1016/j.isprsjprs.2019.09.001

Anfuso, G., and Del Pozo, J. ÁM. (2009). Assessment of coastal vulnerability through the use of GIS tools in South Sicily (Italy). *Environ. Manag.* 43, 533–545. doi: 10.1007/s00267-008-9238-8

Anthony, E. J., Almar, R., Besset, M., Reyns, J., Laibi, R., Ranasinghe, R., et al. (2019). Response of the Bight of Benin (Gulf of Guinea, West Africa) coastline to anthropogenic and natural forcing, Part 2: sources and patterns of sediment supply, sediment cells, and recent shoreline change. *Cont. Shelf Res.* 173, 93–103. doi: 10.1016/j.csr.2018.12.006

Barbaro, G. (2013). Saline Joniche: a predicted disaster. *Disaster Adv.* 6, 1–3. doi: 10.1017/dmp.2020.417

Barbaro, G. (2016). Master Plan of solutions to mitigate the risk of coastal erosion in Calabria (Italy), a case study. *Ocean Coast. Manag.* 132, 24–35. doi: 10.1016/j.ocecoaman.2016.08.001

Barbaro, G., Bombino, G., Foti, G., Borrello, M. M., and Puntorieri, P. (2019a). Shoreline evolution near river mouth: case study of Petrace River (Calabria. Italy). *Reg. Stud. Mar. Sci.* 29:100619. doi: 10.1016/j.rsma.2019.100619

Barbaro, G., Foti, G., Nucera, A., Barillà, G. C., Canale, C., Puntorieri, P., et al. (2020). Risk mapping of coastal flooding areas. Case studies: scilla and Monasterace (Italy). *Int. J. Saf. Secur. Eng.* 10, 59–67. doi: 10.18280/ijsse.100108

Barbaro, G., Foti, G., Sicilia, C. L., and Malara, G. (2014b). A formula for the calculation of the longshore sediment transport including spectral effects. *J. Coast. Res.* 30, 961–966. doi: 10.2112/jcoastres-d-13-00131.1

Barbaro, G., Foti, G., and Sicilia, C. L. (2014a). Coastal erosion in the South of Italy. *Disaster Adv.* 7, 37–42.

Barbaro, G., Petrucci, O., Canale, C., Foti, G., Mancuso, P., and Puntorieri, P. (2019b). "Contemporaneity of floods and storms. A case study of Metropolitan Area of Reggio Calabria in Southern Italy," in *New Metropolitan Perspectives (NMP) (Reggio Calabria, Italy), Smart Innovation, Systems and Technologies*, Vol. 101, eds F. Calabrò, L. Della Spina, and C. Bevilacqua (Cham: Springer), 614–620. doi: 10.1007/978-3-319-92102-0_66

Barnard, P. L., Short, A. D., Harley, M. D., Splinter, K. D., Vitousek, S., Turner, I. L., et al. (2015). Coastal vulnerability across the Pacific dominated by El Nino/Southern oscillation. *Nat. Geosci.* 8, 801–807. doi: 10.1038/ngeo2539

Besset, M., Anthony, E. J., and Bouchette, F. (2019). Multi-decadal variations in delta shorelines and their relationship to river sediment supply: an assessment and review. *Earth Sci. Rev.* 193, 199–219. doi: 10.1016/j.earscirev.2019.04.018

Bird, E. (2018). "). Coastline changes," in *Encyclopedia of Coastal Science. Encyclopedia of Earth Sciences Series*, eds C. Finkl and C. Makowski (Cham: Springer), doi: 10.1007/978-3-319-48657-4_93-2

Boak, E. H., and Turner, I. L. (2005). Shoreline definition and detection: a review. *J. Coast. Res.* 21, 688–703. doi: 10.2112/03-0071.1

Bruno, M. F., Saponieri, A., Molfetta, M. G., and Damiani, L. (2020). The DPSIR approach for coastal risk assessment under climate change at regional scale: the case of apulian coast (Italy). *J. Mar. Sci. Eng.* 8:531. doi: 10.3390/jmse8070531

Canale, C., Barbaro, G., Foti, G., Petrucci, O., Besio, G., and Barillà, G. C. (2021). Bruzzano river mouth damage to meteorological events. *Int. J. River Basin Manag.* 1–17. doi: 10.1080/15715124.2021.1901725

Canale, C., Barbaro, G., Petrucci, O., Fiamma, V., Foti, G., Barillà, G. C., et al. (2020). Analysis of floods and storms: concurrent conditions. *Ital. J. Eng. Geol. Environ.* 1, 23–29. doi: 10.1016/j.envpol.2018.01.104

Dada, O. A., Li, G., Qiao, L., Asiwaju-Bello, Y. A., and Anifowose, A. Y. B. (2018). Recent Niger Delta shoreline response to Niger River Hydrology: conflicts between forces of Nature and Humans. *J. Afr. Earth Sci.* 139, 222–231. doi: 10.1016/j.jafrearsci.2017.12.023

Dada, O. A., Qiao, L., Ding, D., Li, G., Ma, Y., and Wang, L. (2015). Evolutionary trends of the Niger Delta shoreline during the last 100 years: responses to rainfall and river discharge. *Mar. Geol.* 367, 202–211. doi: 10.1016/j.margeo.2015.06.007

Del Rio, L., and Garcia, F. J. (2013). Error determination in the photogrammetric assessment of shoreline changes. *Natural Hazard.* 65, 238–2397. doi: 10.1007/s11069-012-0407-y

Duarte, C. R., De Miranda, F. P., Landau, L., Souto, M. V. S., Sabadia, J. A. B., Da Silva, C. A., et al. (2018). Short-time analysis of shoreline based on RapidEye satellite images in the terminal area of Pecem Port, Ceara, Brazil. *Int. J. Remote Sens.* 39, 4376–4389. doi: 10.1080/01431161.2018.1457229

Ferreira Silva, S., Martinho, M., Capitao, R., Reis, T., Fortes, C. J., and Ferreira, J. C. (2017). An index-based method for coastal-flood risk assessment in low-lying areas (Costa de Caparica. Portugal). *Ocean Coast. Manag.* 144, 90–104. doi: 10.1016/j.ocecoaman.2017.04.010

Fiori, E., Comellas, A., Molini, L., Rebora, N., Siccardi, F., Gochis, D. J., et al. (2014). Analysis and hindcast simulations of an extreme rainfall event in the Mediterranean area: the Genoa 2011 case. *Atmosp. Res.* 138, 13–29. doi: 10.1016/j.atmosres.2013.10.007

Foti, G., Barbaro, G., Barillà, G. C., and Frega, F. (2022). Effects of anthropogenic pressures on dune systems—case study: calabria (Italy). *J. Mar. Sci. Eng.* 10:10. doi: 10.3390/jmse10010010

Foti, G., Barbaro, G., Bombino, G., Fiamma, V., Puntorieri, P., Minniti, F., et al. (2019). Shoreline changes near river mouth: case study of Sant'Agata River

(Reggio Calabria, Italy). *Eur. J. Remote Sens.* 52(Suppl.4), 102–112. doi: 10.1080/22797254.2019.1686955

Foti, G., Barbaro, G., Manti, A., Foti, P., La Torre, A., Geria, P. F., et al. (2020a). A methodology to evaluate the effects of river sediment withdrawal: the case study of the Amendolea River in Southern Italy. *Aquat. Ecosyst. Health Manag.* 23:465. doi: 10.1080/14634988.2020.1807248

Foti, G., Barillà, G. C., Barbaro, G., and Puntorieri, P. (2020b). Remote sensing and GIS to support coastal erosion risk analysis in Calabria (Italy). *WIT Trans. Eng. Sci.* 129, 67–76. doi: 10.2495/risk200061

Goncalves, R. M., Saleem, A., Queiroz, H. A., and Awange, J. L. (2019). A fuzzy model integrating shoreline changes, NDVI and settlement influences for coastal zone human impact classification. *Appl. Geogr.* 113:102093. doi: 10.1016/j.apgeog.2019.102093

Görmüş, T., Ayat, B., Aydoǒan, B., and Tătui, F. (2021). Basin scale spatiotemporal analysis of shoreline change in the Black Sea. *Estuar. Coast. Shelf Sci.* 252:107247. doi: 10.1016/j.ecss.2021.107247

Hagenaars, G., de Vries, S., Luijendijk, A. P., de Boer, W. P., and Reniers, A. J. H. M. (2018). On the accuracy of automated shoreline detection derived from satellite imagery: a case study of the Sand Motor mega-scale nourishment. *Coast. Eng.* 133, 113–125. doi: 10.1016/j.coastaleng.2017.12.011

Hapke, C. J., Himmelstoss, E. A., Kratzmann, M. G., List, J. H., and Thieler, E. R. (2010). *National Assessment of Shoreline Change: Historical Shoreline Change along the New England and Mid-Atlantic Coasts. Open-File Report 1118*. Reston, VA: US Geological Survey, doi: 10.3133/ofr20101118

Harley, M. D., Turner, I. L., Kinsela, M. A., Middleton, J. H., Mumford, P. J., Splinter, K. D., et al. (2017). Extreme coastal erosion enhanced by anomalous extratropical storm wave direction. *Sci. Rep.* 7:6033. doi: 10.1038/s41598-017-05792-1

IPCC (2013). "Climate change 2013: the physical science basis," in *Contribution of Working Group I to the Fifth Assessment Report of the Intergovernmental Panel on Climate Change*, eds T. F. Stocker, D. Qin, G.-K. Plattner, M. Tignor, S. K. Allen, J. Boschung, et al. (Cambridge: Cambridge University Press).

IPCC (2021). "Summary for Policymakers," in *Climate Change 2021: The Physical Science Basis. Working Group I contribution to the Sixth Assessment Report of the Intergovernmental Panel on Climate Change*, eds V. Masson-Delmotte, P. Zhai, A. Pirani, S. L. Connors, C. Péan, S. Berger, et al. (Cambridge: Cambridge University Press).

Istituto Idrografico della Marina (2020). *Tavole di Marea e Delle Correnti di Marea*. Genova: Istituto Idrografico della Marina Italiana.

Jaranovic, B., Trindade, J., Ribeiro, J., and Silva, A. (2017). Using a coastal storm hazard index to assess storm impacts in Lisbon. *Int. J. Saf. Secur. Eng.* 7, 221–233. doi: 10.2495/safe-v7-n2-221-233

Kantamaneni, K., Phillips, M., Thomas, T., and Jenkins, R. (2018). Assessing coastal vulnerability: development of a combined physical and economic index. *Ocean Coast. Manag.* 158, 164–175. doi: 10.1016/j.ocecoaman.2018.03.039

Komar, P. D. (2000). Coastal erosion–underlying factors and human impacts. *Shore Beach* 68, 3–16.

Konlechner, T. M., Kennedy, D. M., O'Grady, J. J., Leach, C., Ranasinghe, R., Carvalho, R. C., et al. (2020). Mapping spatial variability in shoreline change hotspots from satellite data; a case study in southeast Australia. *Estuar. Coast. Shelf Sci.* 246:107018. doi: 10.1016/j.ecss.2020.107018

Kroon, A., de Schipper, M. A., van Gelder, P. H. A. J. M., and Aarninkhof, S. G. J. (2020). Ranking uncertainty: wave climate variability versus model uncertainty in probabilistic assessment of coastline change. *Coast. Eng.* 158:103673. doi: 10.1016/j.coastaleng.2020.103673

Le Mauff, B., Juigner, M., Ba, A., Robin, M., Launeau, P., and Fattal, P. (2018). Coastal monitoring solutions of the geomorphological response of beach-dune systems using multi-temporal LiDAR datasets (Vendée coast. France). *Geomorphology* 304, 121–140. doi: 10.1016/j.geomorph.2017.12.037

Li, X., Zhou, Y., Zhang, L., and Kuang, R. (2014). Shoreline change of Chongming Dongtan and response to river sediment load: a remote sensing assessment. *J. Hydrol.* 511, 432–442. doi: 10.1016/j.jhydrol.2014.02.013

Luijendijk, A., Hagenaars, G., Ranasinghe, R., Baart, F., Donchyts, G., and Aarninkhof, S. (2018). The state of the world's beaches. *Sci. Rep.* 8:6641. doi: 10.1038/s41598-018-24630-6

Maanan, M., and Robin, M. (2010). *Geomatic Solutions for Coastal Environments*. Hauppauge, NY: Nova Science Pub Inc.

Maiti, S., and Bhattacharya, A. K. (2009). Shoreline change analysis and its application to prediction: a remote sensing and statistics based approach. *Mar. Geol.* 257, 11–23. doi: 10.1016/j.margeo.2008.10.006

Mao, Y., Harris, D. L., Xie, Z., and Phinn, S. (2021). Efficient measurement of large-scale decadal shoreline change with increased accuracy in tide-dominated coastal environments with Google Earth Engine. *ISPRS J. Photogramm. Remote Sens.* 181, 385–399. doi: 10.1016/j.isprsjprs.2021.09.021

Mavromatidi, A., Briche, E., and Claeys, C. (2018). Mapping and analyzing socio-environmental vulnerability to coastal hazards induced by climate change: an application to coastal Mediterranean cities in France. *Cities* 72, 189–200. doi: 10.1016/j.cities.2017.08.007

McLaughlin, S., and Cooper, J. A. G. (2010). A multi-scale coastal vulnerability index: a tool for coastal managers? *Environ. Hazards* 9, 233–248. doi: 10.3763/ehaz.2010.0052

Mentaschi, L., Vousdoukas, M. I., Pekel, J. F., Voukouvalas, E., and Feyen, L. (2018). Global long-term observations of coastal erosion and accretion. *Sci. Rep.* 8:12876. doi: 10.1038/s41598-018-30904-w

Miduri, M., Foti, G., and Puntorieri, P. (2017). "Impact generated by Marina of Badolato (Italy) on adjacent coast," in *In Proceedings of the 13th International Congress on Coastal and Marine Sciences, Engineering, Management and Conservation MEDCOAST*, Vol. 2 (Mellieha), 935–945.

Mills, J. P., Buckley, S. J., Mitchell, H. L., Clarke, P. J., and Edwards, J. (2005). A geomatics data integration technique for coastal change monitoring. *Earth Surf. Process. Landf.* 30, 651–664. doi: 10.1002/esp.1165

Mucerino, L., Albarella, M., Carpi, L., Besio, G., Benedetti, A., Corradi, N., et al. (2019). Coastal exposure assessment on Bonassola bay. *Ocean Coast. Manag.* 167, 20–31. doi: 10.1016/j.ocecoaman.2018.09.015

Narra, P., Coelho, C., Sancho, F., and Palalane, J. (2017). CERA: an open-source tool for coastal erosion risk assessment. *Ocean Coast. Manag.* 142, 1–14. doi: 10.1016/j.ocecoaman.2017.03.013

Nerem, R. S., Beckley, B. D., Fasullo, J. T., Hamlington, B. D., Masters, D., and Mitchum, G. T. (2018). Climate-change–driven accelerated sea-level rise detected in the altimeter era. *Proc. Natl. Acad. Sci. U.S.A.* 115, 2022–2025. doi: 10.1073/pnas.1717312115

Ngowo, R. G., Ribeiro, M. C., and Pereira, M. J. (2021). Quantifying 28-year (1991–2019) shoreline change trends along the Mnazi Bay–Ruvuma Estuary Marine Park, Tanzania. *Remote Sens. Appl. Soc. Environ.* 23:100607. doi: 10.1016/j.rsase.2021.100607

Nicolae-Lerma, A., Ayache, B., Ulvoas, B., Paris, F., Bernon, N., Bultreau, T., et al. (2019). Pluriannual beach-dune evolutions at regional scale: erosion and recovery sequences analysis along the Aquitaine coast based on airborne LiDAR data. *Cont. Shelf Res.* 189:103974. doi: 10.1016/j.csr.2019.103974

Ozpolat, E., and Demir, T. (2019). The spatiotemporal shoreline dynamics of a delta under natural and anthropogenic conditions from 1950 to 2018: a dramatic case from the Eastern Mediterranean. *Ocean Coast. Manag.* 180:104910. doi: 10.1016/j.ocecoaman.2019.104910

Pantusa, D., D'Alessandro, F., Riefolo, L., Principato, F., and Tomasicchio, G. R. (2018). Application of a coastal vulnerability index. A case study along the Apulian Coastline, Italy. *Water* 10:1218. doi: 10.3390/w10091218

Prumm, M., and Iglesias, G. (2016). Impacts of port development on estuarine morphodynamics: Ribadeo (Spain). *Ocean Coast. Manag.* 130, 58–72. doi: 10.1016/j.ocecoaman.2016.05.003

Qiao, G., Mi, H., Wang, W., Tong, X., Li, Z., Li, T., et al. (2018). 55-year (1960–2015) spatiotemporal shoreline change analysis using historical DISP and Landsat time series data in Shanghai. *Int. J. Appl. Earth Obs. Geoinform.* 68, 238–251. doi: 10.1016/j.jag.2018.02.009

Ramieri, E., Hartley, A., Barbanti, A., Santos, F. D., Gomes, A., Hilden, M., et al. (2012). Estimating coastal recession due to sea level rise: beyond the Bruun rule. *Clim. Chang.* 110, 561–574. doi: 10.1007/s10584-011-0107-8

Ranasinghe, R., McLoughlin, R., Short, A., and Symonds, G. (2004). The Southern Oscillation Index, wave climate, and beach rotation. *Mar. Geol.* 204, 273–287. doi: 10.1016/s0025-3227(04)00002-7

Sabato, L., and Tropeano, M. (2014). Fiumara: a kind of high hazard river. *Phys. Chem. Earth* 29, 707–715. doi: 10.1016/j.pce.2004.03.008

Sannino, G., Carillo, A., Pisacane, G., and Naranjo, C. (2015). On the relevance of tidal forcing in modeling the Mediterranean thermohaline circulation. *Prog. Oceanogr.* 134, 304–329. doi: 10.1016/j.pocean.2015.03.002

Santini, M. (2011). Methods for assessing coastal vulnerability to climate change. *ETC CCA Techn. Pap.* 1, 1–93.

Satta, A., Puddu, M., Venturini, S., and Giupponi, C. (2017). Assessment of coastal risks to climate change related impacts at regional scale: the case of Mediterranean region. *Int. J. Disaster Risk Reduct.* 24, 284–296. doi: 10.1016/j.ijdrr.2017.06.018

Satta, A., Snoussi, M., Puddu, M., Flayou, L., and Hoult, R. (2016). An index-based method to assess risks of climate-related hazards in coastal zones: the case of Tetouan. *Estuar. Coast. Shelf Sci.* 175, 93–105. doi: 10.1016/j.ecss.2016.03.021

Short, A. D., and Trembanis, A. C. (2004). Decadal scale patterns in beach oscillation and rotation Narrabeen Beach, Australia—time series, PCA and wavelet analysis. *J. Coast. Res.* 202, 523–532. doi: 10.2112/1551-5036(2004)020[0523:dspibo]2.0.co;2

Sorriso-Valvo, M., and Terranova, O. (2006). The Calabrian fiumara streams. *Z. Geomorphol.* 143, 109–125.

Thomas, T., Phillips, M. R., Williams, A. T., and Jenkins, R. E. (2011). Short-term beach rotation, wave climate and the North Atlantic Oscillation (NAO). *Prog. Phys. Geogr. Earth Environ.* 35, 333–352. doi: 10.1177/0309133310397415

Tomasicchio, G. R., D'Alessandro, F., Barbaro, G., Musci, E., and De Giosa, T. M. (2015). Longshore transport at shingle beaches: an independent verification of the general model. *Coast. Eng.* 104, 69–75. doi: 10.1016/j.coastaleng.2015.07.003

Torresan, S., Critto, A., Rizzi, J., and Marcomini, A. (2012). Assessment of coastal vulnerability to climate change hazards at the regional scale: the case study of the North Adriatic Sea. *Natural Hazards Earth Syst. Sci.* 12, 2347–2368. doi: 10.5194/nhess-12-2347-2012

Toure, S., Diop, O., Kpalma, K., and Maiga, A. S. (2019). Shoreline detection using optical remote sensing: a review. *ISPRS Int. J. GeoInform.* 8:75. doi: 10.3390/ijgi8020075

Turner, I. L. (2006). Discriminating Modes of Shoreline Response to Offshore-Detached Structures. *J. Waterway Port Coast. Ocean Eng.* 132, 180–191. doi: 10.1061/(asce)0733-950x2006132:3(180)

Valsamidis, A., and Reeve, D. E. (2017). Modelling shoreline evolution in the vicinity of a groyne and a river. *Cont. Shelf Res.* 132, 49–57. doi: 10.1016/j.csr.2016.11.010

Viavattene, C., Jiménez, J. A., Ferreira, O., Priest, S., Owen, D., and McCall, R. (2018). Finding coastal hotspots of risk at the regional scale: the coastal risk assessment framework. *Coast. Eng.* 134, 33–47. doi: 10.1016/j.coastaleng.2017.09.002

Vos, K., Harley, M. D., Splinter, K. D., Simmons, J. A., and Turner, I. L. (2019). Sub-annual to multi-decadal shoreline variability from publicly available satellite imagery. *Coast. Eng.* 150, 160–174. doi: 10.1016/j.coastaleng.2019.04.004

Wang, J., Zhou, W., Pickett, S. T., Yu, W., and Li, W. (2019). A multiscale analysis of urbanization effects on ecosystem services supply in an urban megaregion. *Sci. Total Environ.* 662, 824–833. doi: 10.1016/j.scitotenv.2019.01.260

Williams, A. T., Rangel-Buitrago, N., Pranzini, E., and Anfuso, G. (2018). The management of coastal erosion. *Ocean Coast. Manag.* 156, 4–20. doi: 10.1016/j.ocecoaman.2017.03.022

Yang, Z., Wang, T., Voisin, N., and Copping, A. (2015). Estuarine response to river flow and sea-level rise under future climate change and human development. *Estuar. Coast. Shelf Sci.* 156, 19–30. doi: 10.1016/j.ecss.2014.08.015

Zellou, B., and Rahali, H. (2019). Assessment of the joint impact of extreme rainfall and storm surge on the risk of flooding in a coastal area. *J. Hydrol.* 569, 647–665. doi: 10.1016/j.jhydrol.2018.12.028

Zema, D. A., Bombino, G., Boix-Fayos, C., Tamburino, V., Zimbone, S. M., and Fortugno, D. (2014). Evaluation and modeling of scouring and sedimentation around check dams in a Mediterranean torrent in Calabria, Italy. *J. Soil Water Conserv.* 69, 316–329. doi: 10.2489/jswc.69.4.316

Zhai, T., Wang, J., Fang, Y., Qin, Y., Huang, L., and Chen, Y. (2020). Assessing ecological risks caused by human activities in rapid urbanization coastal areas: towards an integrated approach to determining key areas of terrestrial-oceanic ecosystems preservation and restoration. *Sci. Total Environ.* 708:135153. doi: 10.1016/j.scitotenv.2019.135153

Zhang, R., Chen, L., Liu, S., Zhang, H., Gong, W., and Lin, G. (2019). Shoreline evolution in an embayed beach adjacent to tidal inlet: the impact of anthropogenic activities. *Geomorphology* 346:106856. doi: 10.1016/j.geomorph.2019.106856

Conflict of Interest: The authors declare that the research was conducted in the absence of any commercial or financial relationships that could be construed as a potential conflict of interest.

Publisher's Note: All claims expressed in this article are solely those of the authors and do not necessarily represent those of their affiliated organizations, or those of the publisher, the editors and the reviewers. Any product that may be evaluated in this article, or claim that may be made by its manufacturer, is not guaranteed or endorsed by the publisher.